ELSEVIER

www.elsevier.nl/locate/carres

Carbohydrate Research 333 (2001) 7–17

CARBOHYDRATE RESEARCH

The identification of the catalytic nucleophiles of two β-galactosidases from glycoside hydrolase family 35

Jan E. Blanchard,[a] Laurent Gal,[b] Shouming He,[a] Janine Foisy,[b] R. Antony J. Warren,[b] Stephen G. Withers[a,*]

[a]*Department of Chemistry, Protein Engineering Network of Centres of Excellence of Canada, University of British Columbia, Vancouver, BC, Canada V6T 1Z1*

[b]*Department of Microbiology, Protein Engineering Network of Centres of Excellence of Canada, University of British Columbia, Vancouver, BC, Canada V6T 1Z1*

Received 26 February 2001; accepted 9 April 2001

Abstract

The β-galactosidases from *Xanthomonas manihotis* (β-Gal Xmn) and *Bacillus circulans* (β-Gal-3 Bcir) are retaining glycosidases that hydrolyze glycosidic bonds through a double displacement mechanism involving a covalent glycosyl–enzyme intermediate. The mechanism-based inactivator 2,4-dinitrophenyl 2-deoxy-2-fluoro-β-D-galactopyranoside was shown to inactivate β-Gal Xmn and β-Gal-3 Bcir through the accumulation of 2-deoxy-2-fluorogalactosyl enzyme intermediates with half lives of 40 and 625 h, respectively. Peptic digestion of these labeled enzymes and analysis by LC–MS identified Glu^{260} and Glu^{233} as the catalytic nucleophiles involved in the formation of the glycosyl–enzyme intermediate during catalysis by β-Gal Xmn and β-Gal-3 Bcir, respectively. These findings confirm the previous prediction of the position of these residues based on primary sequence similarities to other members of the glycoside hydrolase family 35.

Keywords: Glycosidases; Labeling; Fluorosugars; Galactosidase; Mass spectrometry

1. Introduction

Retaining glycosidases catalyze the cleavage of glycosidic bonds with net retention of anomeric configuration.[1,2] Hydrolysis is catalyzed through a double displacement mechanism, aided by a pair of carboxylic acids strategically placed in the enzyme active site (Scheme 1). In the first step of catalysis (glycosylation), a carboxylate attacks the anomeric center of the scissile bond, while another carboxylic acid side-chain provides general acid catalysis. This step results in the formation of a covalent glycosyl–enzyme intermediate that subsequently undergoes deglycosylation by the general base-catalyzed nucleophilic attack of either water (hydrolysis) or another moiety (transglycosylation).

The natural ability of glycosidases to transglycosylate can be exploited to synthesize glycosidic bonds. Although this method of transglycosylation has been used successfully to synthesize a number of different linkages,[3–6] there are still drawbacks to this methodology, including the subsequent hydrolysis of transglycosylation products by the glycosidase. The recent development of glycosynthases[7–10] circumvents this problem; these are glycosidases in which the amino acid

* Corresponding author. Tel.: +1-604-8223266; fax: +1-604-8222847.

E-mail address: withers@chem.ubc.ca (S.G. Withers).

0008-6215/01/$ - see front matter
PII: S0008-6215(01)00108-2

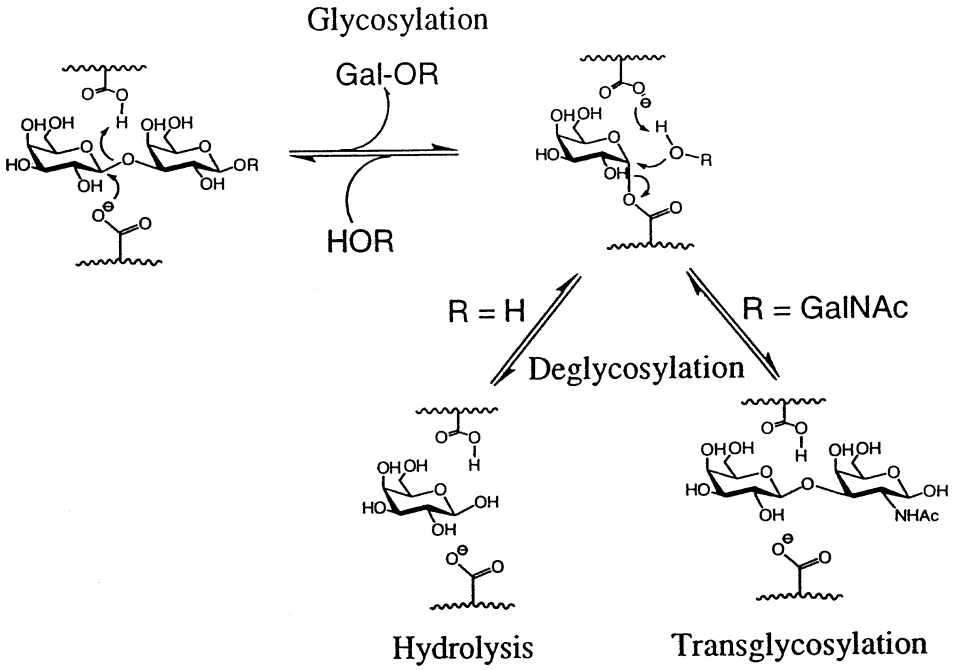

Scheme 1. The mechanism of catalysis of a retaining β-galactosidase.

residue responsible for nucleophilic catalysis has been specifically substituted to a non-nucleophilic residue, typically alanine or serine. If a glycosyl fluoride donor with the anomeric configuration opposite to that of the natural substrate is supplied, along with a suitable acceptor, transglycosylation can occur in high yields (90–100%).

The first step in the construction of a glycosynthase is the identification of the residue responsible for nucleophilic catalysis for a given glycosidase. This can be achieved through a methodology that involves labeling the residue of interest with a fluoro-glycoside. Glycosides substituted with fluorine at the C-2 or C-5 position have been demonstrated to be excellent mechanism-based inactivators of glycosidases.[11,12] The fluorine substituent destabilizes the oxacarbenium ion-like transition states associated with glycosylation and deglycosylation, thereby slowing both steps of catalysis. A good leaving group at the anomeric center, such as dinitrophenyl or fluoride, accelerates glycosylation relative to deglycosylation, resulting in the accumulation of the glycosyl–enzyme intermediate, thereby rendering the enzyme inactive. This trapped glycosyl–enzyme is then digested by a protease, and the resultant peptide fragments analyzed by LC–MS. The peptide covalently attached to the fluoro-glycosyl moiety is identified by comparison to an equivalent digest of non-inactivated enzyme and sequenced to identify the catalytic amino acid residue. To date, this procedure has been used successfully to assign the position of the catalytic nucleophile in a number of glycosidases.[13–17]

The β-galactosidase from the pathogenic bacterium *Xanthomonas manihotis* (EC 3.2.1.23, AC P48982; β-Gal Xmn) is a 66 kDa exoglycosidase that hydrolyzes (1→3) and, to a lesser degree, (1→4) terminally linked galactose residues from oligosaccharides.[18,19] β-Gal Xmn has a strong sequence similarity (42% identity, 57% similarity) to a 67 kDa (1→3) β-galactosidase from *Bacillus circulans* (EC 3.2.1.23, AC O31341; β-Gal-3 Bcir), the third β-galactosidase to be isolated from this bacterium.[20] The recently developed classification system that assigns glycosidases into groups based on primary amino acid sequence similarities,[21–23] designates β-Gal Xmn and β-Gal-3 Bcir as family 35 enzymes.[†] This is a relatively diverse family, containing over 25 retaining β-galactosidases, the vast majority of which are eukaryotic in origin, including the

[†] http://afmb.cnrs-mrs.fr/ ~ pedro/CAZY/ghf_35.html.

human lysosomal enzyme. Mutations at several sites in this glycosidase result in the neurological disorders GM1-gangliosidosis and Morquio B. syndrome.[24] To date, there are only four bacterial members of family 35: β-Gal Xmn, β-Gal-3 Bcir, and β-galactosidases from *Arthrobacter sp.*[25] and *Streptomyces coelicolor*.[26] Due to the similarity between β-Gal Xmn, β-Gal-3 Bcir, and the human enzyme, mechanistic or structural studies of the more readily studied β-Gal Xmn and β-Gal-3 Bcir are of particular interest as they could contribute to an understanding of the human β-galactosidase and its associated disorders. In addition, since β-Gal Xmn and β-Gal-3 Bcir, in common with the mammalian enzyme, preferentially hydrolyze $(1\rightarrow3)$ linkages, glycosynthases engineered from these glycosidases are likely to be able to synthesize these same linkages. 2-Acetamido-2-deoxy-3-*O*-(β-D-galactopyranosyl)-D-glucopyranose plays an integral role in complex carbohydrates in vivo and is therefore a desirable target for the synthesis of carbohydrate conjugates for study. Although this target has been synthesized via transglycosylation by β-Gal Xmn[27] and β-Gal-3 Bcir,[28] as well as bovine testes β-galactosidase,[29] yields were relatively low (12–22%). The use of β-Gal Xmn and β-Gal-3 Bcir as glycosynthases would hopefully greatly improve these yields and thereby expand the range of application. This approach therefore requires prior knowledge of the identity of the nucleophile within each enzyme sequence. This key catalytic residue has previously been identified within the human β-galactosidase;[13] however, given the diversity of this family, it seemed wise to confirm the identity of the nucleophile in enzymes from a prokaryotic source.

This paper describes the inactivation of β-Gal Xmn and β-Gal-3 Bcir by 2,4-dinitrophenyl 2-deoxy-2-fluoro-β-D-galactopyranoside (2FDNPGal) and subsequent experimental identification of the catalytic nucleophiles of these glycosidases.

2. Experimental

General.—All buffers, substrates, and reagents were purchased from either Sigma–Aldrich Co. or Aldrich Chemical Company unless noted otherwise. *Pwo* DNA polymerase and deoxynucleoside triphosphates were from Boehringer Mannheim. Restriction endonucleases, Vent polymerase, and T4 DNA ligase were from New England Biolabs (NEB). Galactosyl-imidazole was a gift from Dr Andrea Vasella (Institut für Organische Chemie, ETH-Zürich). Protein sequence alignments were done with the National Center for Biotechnology Information (NCBI) BLAST server site.[30‡] Preparation of oligonucleotide primers, and DNA and protein sequencing was performed by the Nucleic Acid-Protein Service Unit, University of British Columbia. Curve fitting was done with GRAFIT.[31] Enzyme activity assays were performed on a Unicam UV4 UV–Vis spectrometer; the spectrometer and cuvettes were pre-equilibrated to 37 °C by the use of a circulating water bath. Polystyrol or acryl 1-mL disposable cuvettes were used for all spectrometer measurements.

Construction of His_6-tagged β-Gal Xmn.—The gene encoding β-Gal Xmn minus the amino-terminal 21 amino acid signal sequence coding region (pCTβ-Gal-100) was obtained as a construct in vector pAGR3 (NEB) from Dr Christopher Taron (Department of Biochemistry, University of Illinois at Urbana-Champaign). The β-Gal Xmn gene was subcloned into pTUG10N18 using the *Hind*III and *Nco*I restriction sites. This new pTUG10N18/β-Gal construct (52 ng) was used as the template in PCR with 21 pmol oligonucleotide primers (see below), 200 μmol of each of the four deoxynucleoside triphosphates and 5% Me_2SO in 50 μL of Vent polymerase buffer. The mixture was heated at 96 °C for 60 s and 5 U of Vent polymerase added to start the reaction. Twenty-five PCR cycles (95 °C for 30 s, 55 °C for 30 s, 72 °C for 70 s) were performed in a thermal cycler (Perkin–Elmer, GeneAmp PCR System 2400). Primers were as follows: 5′-GTG GAA AAC AGC GGC CGC ATC AAT-3′ (forward primer) and 5′-AG TCT AAG CTT GCT AGC TTA GTG ATG GTG ATG GTG ATG GCC GCG CAC GCT GGG GTG-3′ (reverse primer). The PCR product and the

‡ http://www.ncbi.nlm.nih.gov/BLAST.

pTUG10N18/β-Gal construct were each digested with *Hind*III and *Not*I and ligated.

Construction of His$_6$-tagged β-Gal-3 Bcir.—The β-Gal-3 Bcir gene was amplified by PCR with genomic *B. circulans* ATCC31382 DNA (prepared by the method of Ref. 32) as the template (250 μg) and oligonucleotide primers complementary to the *Xho*I and *Nde*I restriction sites (200 nM) with 250 μM of each of the four deoxynucleoside triphosphates in 100 μL of *Pwo* polymerase buffer. The mixture was heated at 95 °C for 120 s and 5 U of *Pwo* polymerase added to start the reaction. Twenty-five PCR cycles (94 °C for 30 s, 59 °C for 45 s, 72 °C for 90 s) were performed in a thermal cycler (Perkin–Elmer, GeneAmp PCR System 2400). The 1760 bp PCR product was ligated into the expression vector pET29b(+) (Novagen) using the *Xho*I and *Nde*I cloning sites.

Expression of β-Gal Xmn and β-Gal-3 Bcir.—The constructs encoding the β-Gal Xmn and β-Gal-3 Bcir genes were each transformed into *Escherichia coli* JM101[33] via electroporation. A single colony grown on Luria-Bertani/ampicillin media was used to inoculate a 30 mL Typ/Amp starter culture (16 g/L tryptone, 16 g/L yeast extract, 5 g/L NaCl, 100 μg ampicillin, pH 7.0). After incubation for 5.5 h at 37 °C, the starter culture was used to inoculate a 2 L Typ/Amp culture. After incubation at 30 °C for 3 h, isopropyl β-D-thiogalactoside was added to a final concentration of 0.1 mM, and the culture was incubated at 30 °C until $OD_{600} = 0.5$. The cells were harvested and spun at 4 °C for 15 min at 10,000*g* to produce the cell paste.

Purification of β-Gal Xmn.—The cell paste was suspended in 50 mM sodium phosphate buffer, 0.5 M NaCl, pH 6.0 (start buffer) (3.8 mL/g), PMSF (0.25 mM) and β-mercaptoethanol (6.7 mM) and the suspension was French pressed three times. The lysed cells were centrifuged at 10,000*g* for 1 h and the supernatant filtered through a 45 μm membrane (final volume ca. 45 mL). The clarified supernatant was loaded onto a Pharmacia Biotech Chelating Sepharose Fast Flow column (18 mL) charged with Ni^{2+} according to the manufacturer's instructions. β-Gal Xmn was eluted using a linear gradient of 0–100 mM imidazole in start buffer. Fractions that showed β-galactosidase activity (determined as described below) were pooled ($V_T = 130$ mL) and dialyzed against 2×2.5 L of 20 mM sodium phosphate buffer, 50 mM NaCl, pH 6.0 (SP buffer), then concentrated in 30 kDa molecular weight cut-off Amicon Centriprep concentrators and loaded onto two prepacked 5 mL Pharmacia Biotech Hi-Trap SP columns connected in tandem. β-Gal Xmn was eluted with a linear gradient of 50–350 mM NaCl in SP buffer. The purified β-Gal Xmn appeared as a single band on silver-stained SDS–PAGE. Amino-terminal sequencing of the purified enzyme (ATPESW) was consistent with the published sequence.[19]

Purification of β-Gal-3 Bcir.—The purification of β-Gal-3 Bcir from the cell paste was accomplished in a single step with a Ni^{2+}-chelating column, as described for β-Gal Xmn, with the following changes: the start and elution buffers were as stated, but included 1 M sodium phosphate, pH 7.0; pooled fractions that contained β-Gal-3 Bcir were dialyzed against 1 M sodium phosphate buffer, pH 7.0. Purified β-Gal-3 Bcir appeared as a single band on Coomassie stained SDS–PAGE. Amino-terminal sequencing of the purified enzyme (SQLTYDDSF) was consistent with the published sequence.[20]

Measurement of enzyme activity of β-Gal Xmn and β-Gal-3 Bcir.—Enzyme activity using *p*NPGal was determined by monitoring the release of *p*NP at 400 nm (ΔA_{400}/min). Spectrometer cuvettes contained 0.1% BSA (w/v) in 50 mM sodium phosphate buffer, pH 6.0 (buffer A) for β-Gal Xmn or pH 7.0 (buffer B) for β-Gal-3 Bcir. Unless noted otherwise, the activity of β-Gal Xmn and β-Gal-3 Bcir was determined with 1.2 mM and 0.94 mM *p*NPGal, respectively, at 37 °C.

Hydrolysis kinetics.—Reaction rates were determined as described above at a minimum of nine different concentrations of *p*NPGal ranging from 7 to 350 μM. Resultant rates and substrate concentrations were fit to the Michaelis–Menten expression to determine values of K_m and V_{max}. Extinction coefficients for *p*-nitrophenol, 3.32 $mM^{-1}\ cm^{-1}$ (pH 6.0) and 9.05 $mM^{-1}\ cm^{-1}$ (pH 7.0) (as determined by the method of Ref. 34), were used to quantify the maximal reaction rate of each

enzyme. Enzyme concentrations were determined by absorbance at 280 nm, and the extinction coefficients of β-Gal Xmn (1.97 mL mg^{-1} cm^{-1}) and β-Gal-3 Bcir (1.46 mL mg^{-1} cm^{-1}) (as determined by the method of Ref. 35), and molecular weights of 64,849 Da (β-Gal Xmn) and 67,859 Da (β-Gal-3 Bcir) (as determined by mass spectrometry) to calculate pseudo first order rate constants, k_{cat}.

The K_i value for inhibition of β-Gal Xmn by galactosyl-imidazole was determined by measuring rates at five concentrations of *p*NP-Gal (within the range of 7.0–91.0 μM), both in the presence (7.2 nM) and absence of galactosyl-imidazole (P). Total reaction volume was 900 μL, using 9.7 μg of β-Gal Xmn. The data were plotted in a Lineweaver–Burk format and the slopes fit to the expression $K_p = [P]/(\text{slope}_i/\text{slope}_o - 1)$ to derive K_p (where slope_o = slope of the Lineweaver–Burk plot when [P] = zero, and slope_i = slope of the Lineweaver–Burk plot when [P] ≠ zero). The same experiment was performed for β-Gal-3 Bcir (5.0 ng) at zero and 290 nM galactosyl-imidazole in 800 μL buffer B.

Inactivation kinetics.—2FDNPGal (1.15–92.0 μM) in BSA-free buffer A (for β-Gal Xmn) or B (for β-Gal-3 Bcir) (100–200 μL) was incubated in a 20 °C (for β-Gal Xmn) or 37 °C (for β-Gal-3 Bcir) water bath for 5 min. β-Gal Xmn or β-Gal-3 Bcir (0.1–9.7 μg) was added to initiate the reaction. Aliquots (5 μL) of this inactivator mix were removed at various times and residual enzyme activity was assayed as described. The fractional loss in activity at each 2FDNPGal concentration was plotted against time and fit to Eq. (1) (for β-Gal Xmn) or Eq. (2) (for β-Gal-3 Bcir), where v/V_o is the fractional activity at time t, A and C are constants, and k_{inact}^{obs} is the observed rate constant.

$$\frac{v}{V_o} = A(e^{-k_{inact}^{obs}t}) + C \quad (1)$$

$$\frac{v}{V_o} = A(e^{-k_{inact}^{obs}t}) \quad (2)$$

Values of k_{inact}^{obs} so derived for β-Gal Bcir and the corresponding 2FDNPGal concentrations ([I]) were fit to Eq. (3) to determine the inhibitor dissociation constant (K_i) and inactivation rate constant (k_{inact}). Saturation with respect to inhibitor was not achieved with β-Gal Xmn; k_{inact}^{obs} and [I] values were therefore fit to Eq. (4) to derive the ratio K_i/k_{inact}.

$$k_{inact}^{obs} = \frac{k_{inact}[I]}{K_i + [I]} \quad (3)$$

$$\frac{1}{k_{inact}^{obs}} = \frac{1}{[I]}\left(\frac{K_i}{k_{inact}}\right) + \frac{1}{k_{inact}} \quad (4)$$

Protection against inactivation.—Values of k_{inact}^{obs} were determined as described for β-Gal Xmn (20 nM) with 2FDNPGal (46 μM) in BSA-free buffer A (final vol = 100 μL) with zero (k_i^{obs}) and 40 nM (k_{ip}^{obs}) of galactosyl-imidazole. The same experiment was performed for β-Gal-3 Bcir (100 nM) with 2FDNPGal (9.6 μM) in BSA-free buffer B (final vol = 100 μL) with zero and 500 nM galactosyl-imidazole.

Catalytic competence of inactivated species

Generation of the inactivated enzyme. β-Gal Xmn or β-Gal-3 Bcir (2.4–5.5 mg) was incubated with 2FDNPGal (0.20–0.40 mM) in BSA-free buffer A or B, respectively (1 mL), until < 5% of the original activity remained. Each inactivated enzyme mixture was concentrated using a 30 kDa molecular weight cut-off Millipore Ultrafree 0.5 centrifugal filter to a volume of 10–20 μL, and fresh BSA-free buffer A or B added to a final volume of 200 μL. This process of concentration and dilution was repeated until all excess inactivator was removed, as determined by the maintenance of full activity of an aliquot (0.01 mg) of non-inactivated enzyme diluted one half with the inactivated species. The concentration of inactivated enzyme was determined by absorption at 280 nm and used to calculate the maximal activity possible (V_o) if the enzyme was completely active.

Demonstration of catalytic competence. Inactivated enzyme freed from excess inactivator (50–175 μg in 75–100 μL) was incubated at 20 °C (β-Gal Xmn) or 37 °C (β-Gal-3 Bcir) in BSA-free buffer A or B, respectively, and aliquots were removed at various times and assayed as described. The gain in fractional activity was fit to a first order equation

$$\left(\frac{v}{V_o} = A(1 - e^{-k_{hydrol}t})\right)$$

(for β-Gal Xmn) or a linear expression (for β-Gal-3 Bcir). This procedure was repeated for β-Gal Xmn in the presence of 31 mM phenyl β-D-glucopyranoside, and for β-Gal-3 Bcir in the presence of 34 mM 2-deoxy-D-*arabino*-hexopyranose to determine the rate constant for reactivation by transglycosylation (k_{trans}).

Identification of the catalytic nucleophiles of β-Gal Xmn and β-Gal-3 Bcir

Digestion of inactivated enzyme. β-Gal Xmn or β-Gal-3 Bcir (14–100 ng) were incubated with 2FDNPGal (0.2–25.8 mmol) in BSA-free buffer A or B, respectively (vol = 65 μL), until $< 5\%$ of the original activity remained. An aliquot (10 μL) of the inactivated enzyme was frozen and kept at −20 °C until analyzed by LC–MS. Each inactivated species (50 μL) was added to pepsin in a ratio of ca. 12:1 (enzyme:pepsin) in 200 mM sodium phosphate, pH 2.0 (vol = 78 μL). Each digestion was performed at rt for either 2 h (for β-Gal Xmn) or 0.5 h (for β-Gal-3 Bcir); the samples were then frozen and kept at −20 °C until analyzed by mass spectrometry.

Electrospray mass spectrometry. Mass spectra were recorded on a Perkin–Elmer Sciex API 300 triple quadrupole mass spectrometer with an ion spray ion source. The spectrometer was interfaced with a Michrom BioResources Inc. Ultrafast Microprotein Analyzer that separated peptides via reverse phase HPLC. Digested proteins were loaded onto a Reliasil C18 column (1 × 150 mm) equilibrated with solvent A (0.05% trifluoroacetic acid (TFA), 2% MeCN in water). Peptides were eluted using a 0–60% gradient of solvent B over 60 min, followed by 100% solvent B over 2 min (solvent B: 0.045% TFA, 80% MeCN in water). The flow rate was 50 μL/min. Spectra were obtained in the single quadrupole scan mode (LC–MS) or the tandem MS daughter ion scan mode (MS–MS).

In LC–MS, the quadrupole mass analyzer was scanned over a mass to charge ratio (m/z) of 300–2400 Da with a step size of 0.5 Da and a dwell time of 1 ms per step. The ion-source voltage (ISV) was 5 kV and the orifice energy (OR) was 50 V. In MS–MS, the spectra were obtained by selectively introducing one of the parent peptides of m/z 869.0, 951.0, 861.5 or 1025.5 from the first quadrupole (Q1) into the collision cell (Q2) and observing the daughter ions in the third quadrupole (Q3). The scan range of Q3 was 50–1920 Da; step size, dwell time, and OR as above; ISV was 4.8 kV.

3. Results and discussion

β-Gal Xmn and β-Gal-3 Bcir were shown to hydrolyze *p*-nitrophenyl β-D-galactopyranoside (*p*NPGal) with associated parameters of $K_m = 0.050 \pm 0.002$ and 0.021 ± 0.001 mM, and $k_{cat} = 35.8 \pm 0.3$ and 18.3 ± 0.3 s^{-1}, respectively. Incubation of β-Gal Xmn and β-Gal-3 Bcir individually in the presence of 2FDNPGal resulted in a time-dependent decrease of enzyme activity according to pseudo-first order kinetics (Fig. 1(a, b)), behavior that was modeled according to Scheme 2. Inactivation of β-Gal-3 Bcir proceeded to completion, thus data were fit to the expression

$$\frac{v}{V_o} = A(e^{-k_{inact}^{obs} t})$$

to yield pseudo first order rate constants at each inactivator concentration. As can be seen in Fig. 1(a), inactivation of β-Gal Xmn did not proceed to completion, thus data were fit to the expression

$$\frac{v}{V_o} = A(e^{-k_{inact}^{obs} t}) + C$$

Such 'steady state' inactivation has been seen previously[36] and shown to be the result of an inhibited enzyme being reactivated in the presence of excess 2FDNPsugar through transglycosylation over the course of the experiment.

Saturation of β-Gal Xmn with respect to inactivator was not achieved since, at high concentrations of 2FDNPGal, inactivation was too rapid to monitor reliably. Therefore, individual values for K_i and k_{inact} could not be accurately determined; however, the ratio K_i/k_{inact} was calculated to be 17 ± 1 μM min from the double reciprocal plot of Fig. 1(c).

Saturation with respect to inactivator was demonstrated with β-Gal Bcir. Derived values of k_{inact}^{obs} were thus fit with 2FDNPGal concentration to Eq. (3) to determine both k_{inact} (0.10 ± 0.01 s^{-1}) and K_i (0.037 ± 0.005 mM)

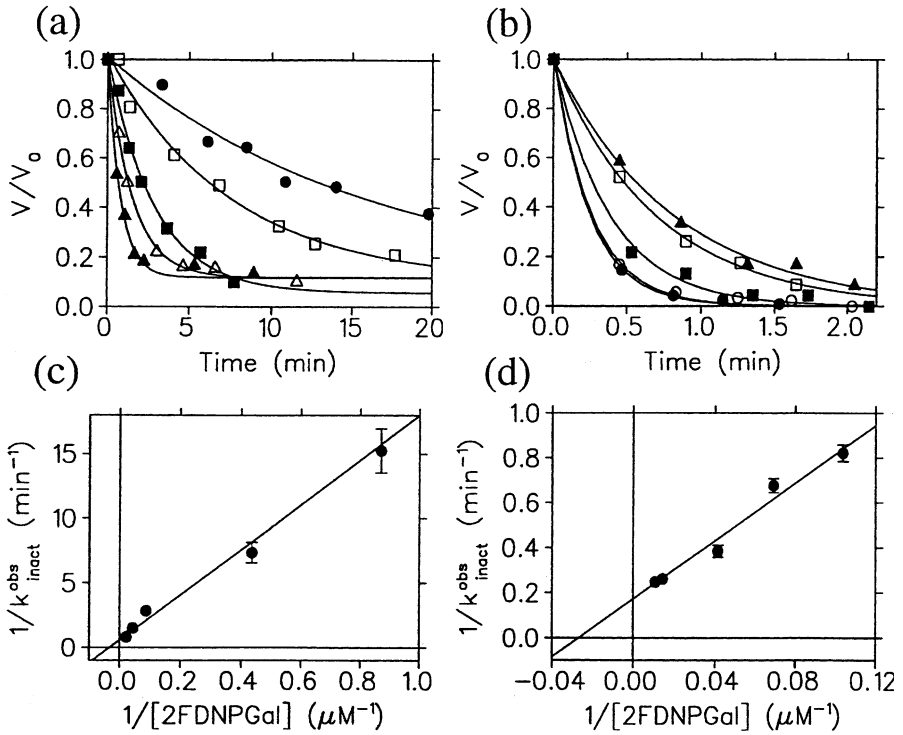

Fig. 1. Inactivation of β-Gal Xmn and β-Gal-3 Bcir by 2FDNPGal. (a) The time-dependent first order decrease in activity of β-Gal Xmn upon incubation with ● 1.15, □ 2.30, ■ 11.5, △ 23.0, and ▲ 46.0 μM 2FDNPGal. (b) The time-dependent first order decrease in activity of β-Gal-3 Bcir upon incubation with ▲ 9.64, □ 14.5, ■ 24.1, ○ 69.0, and ● 92.0 μM 2FDNPGal. (c, d) Double reciprocal plots of observed rate constants versus inhibitor concentration. Note that for β-Gal-3 Bcir, values for k_{inact} and K_i were calculated from a non-linear fit of Eq. (3); panel (d) is for illustrative purposes only.

(Fig. 1(d)). The similarity of the values of K_m for *p*NPGal and K_i for 2FDNPGal suggests that the substitution of a hydroxyl for fluorine at the C-2 position does not significantly affect ground state binding between the enzyme and substrate.

The potent, reversible, competitive inhibitor galacto-configured pyridoimidazole (galactosyl-imidazole) ($K_i = 15$ nM with β-Gal Xmn and $K_i = 220$ nM with β-Gal-3 Bcir) protects β-Gal Xmn and β-Gal-3 Bcir against inactivation by 2FDNPGal. The fractional loss in activity of β-Gal Xmn by 2FDNPGal in the presence and absence of galactosyl-imidazole (Fig. 2(a)) yielded a rate constant ratio (k_{ip}^{obs}/k_i^{obs}) of 0.43, which is in close agreement with the value of 0.48 predicted by Eq. (5) which describes inactivation according to Scheme 2.

$$\frac{k_{ip}^{obs}}{k_i^{obs}} = \frac{K_i + [IX]}{K_i\left(1 + \frac{[P]}{K_p}\right) + [IX]} \quad (5)$$

Similarly, the same experiment performed for β-Gal-3 Bcir (Fig. 2(b)) yielded a rate constant ratio (k_{ip}^{obs}/k_i^{obs}) of 0.42, which is in reasonable agreement with the predicted value of 0.35. The rate of inactivation of both glycosidases by 2FDNPGal decreased by the expected amount in the presence of a competitive inhibitor, data that is consistent with the 2-fluoro-glycoside inactivator being active-site directed.

Once β-Gal Xmn and β-Gal-3 Bcir were inactivated by 2FDNPGal and the excess inhibitor removed, both enzymes spontaneously regained hydrolytic activity over time (Fig. 3). The reactivation data for β-Gal Xmn were fit to a first order equation

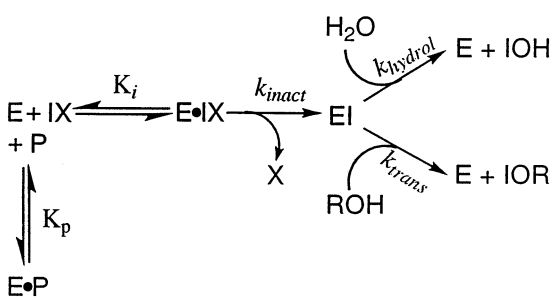

Scheme 2. Enzyme inactivation and reactivation, where E, enzyme; IX, inactivator; and P, competitive inhibitor.

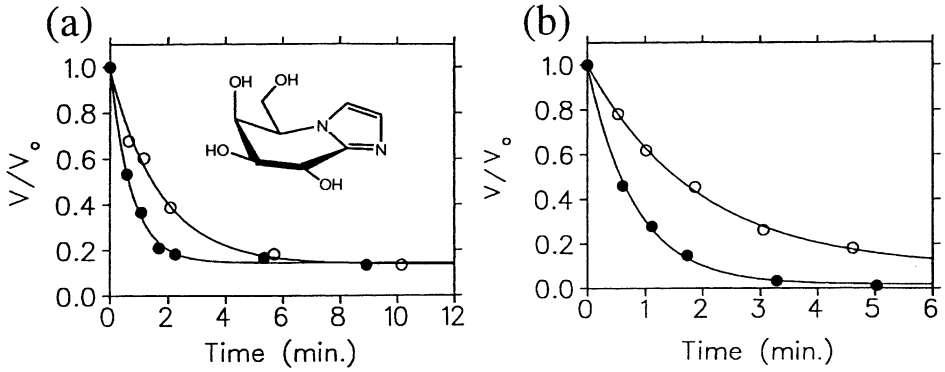

Fig. 2. Protection against inactivation with galactosyl-imidazole. (a) Fractional loss of activity of β-Gal Xmn over time by 46.0 μM 2FDNPGal in the presence ○ and absence ● of 40 nM galactosyl-imidazole (inset). (b) Fractional loss of activity of β-Gal-3 Bcir by 9.6 μM 2FDNPGal in the presence ○ and absence ● of 0.50 μM galactosyl-imidazole.

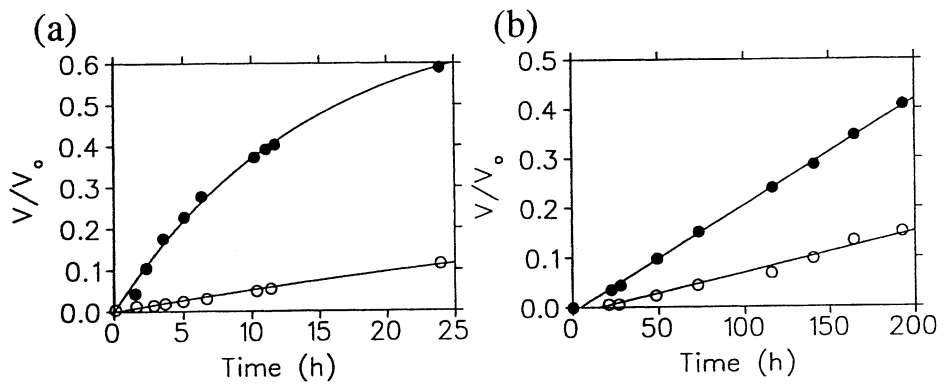

Fig. 3. Reactivation of the trapped intermediates of β-Gal Xmn and β-Gal-3 Bcir. (a) The spontaneous reactivation of 2-deoxy-2-fluorogalactosyl-β-Gal Xmn in the presence ● and absence ○ of 31 mM phenyl β-D-glucopyranoside. (b) The spontaneous reactivation of 2-deoxy-2-fluorogalactosyl-β-Gal-3 Bcir in the presence ● and absence ○ of 34 mM 2-deoxy-D-*arabino*-hexopyranose.

$$\left(\frac{v}{V_o} = A e^{-k_{hydrol} t}\right)$$

to derive a rate constant (k_{hydrol}) of $0.018 \pm 0.001\ h^{-1}$, which corresponds to a half life of 40 h for the glycosyl enzyme intermediate. Data for the reactivation of β-Gal-3 Bcir however, were limited to only the approximately linear portion of the first-order expression. A reliable value for k_{hydrol} could not therefore be extrapolated, but a half life of ≈ 625 h for the trapped intermediate was estimated from Fig. 3(b).

The spontaneous reactivation of each enzyme observed is consistent with the trapping of a catalytically relevant species. Further demonstration of the catalytic competence of the trapped species was provided by the increase in the rate of enzyme reactivation (k_{trans}) in the presence of an acceptor sugar. In the presence of 31 mM phenyl β-D-glucopyranoside, the rate of reactivation of β-Gal Xmn increased fourfold (Fig. 3(a)). Similarly, the reactivation of β-Gal-3 Bcir increased approximately threefold in the presence of 34 mM 2-deoxy-D-*arabino*-hexopyranose. As demonstrated in some detail for a family 1 β-glucosidase,[36] such behavior is entirely consistent with the trapping of a catalytically competent intermediate and then reactivation through transglycosylation.

The stoichiometric reaction of β-Gal Xmn with 2FDNPGal was illustrated by mass spectral analysis. The inactivated enzyme is heavier than the unlabelled enzyme by an amount (171 Da) equivalent, within error, to the expected mass of a 2-fluorogalactosyl moiety (165 Da). The numerous peptide fragments from the digestion of inactivated β-Gal Xmn were separated and detected by HPLC–ESMS as shown in the total ion chromatogram (TIC)

of Fig. 4(a). Comparison of the LC–MS profiles of labeled and unlabelled digests revealed one major difference: a peptide of m/z 869.0 in the control digest, eluting at ca. 28 min, was absent in the labeled digest, but replaced by one of m/z 951.0 that was not present in the control digest (Fig. 4(b, c)).

The difference between the m/z values for these two peptides is 82.0 which is, within

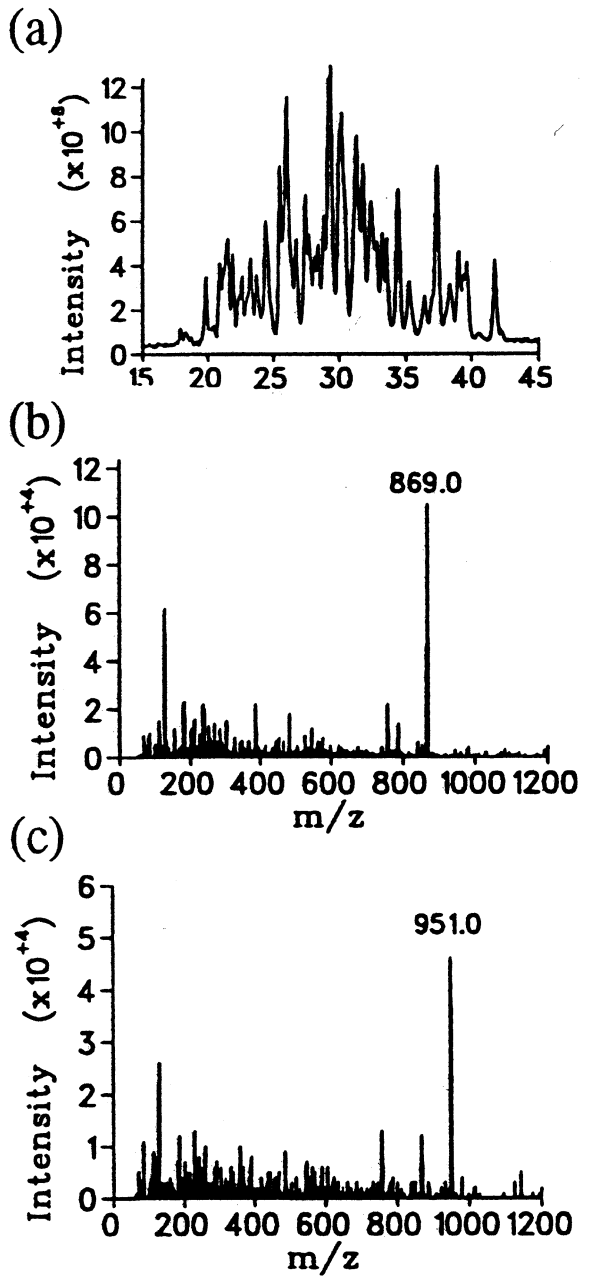

Fig. 4. Detection of the 2-deoxy-2-fluorogalactosyl-β-Gal Xmn species by ESMS. (a) TIC of the control β-Gal Xmn after peptic digestion. Mass spectrum of peptides eluting at ca. 28 min in (b) the control and (c) the labeled digest, showing the m/z values of the major species.

error, one half of the expected mass increase (165 Da), suggesting that these peptides are doubly charged. Hence, $(951.0 \times 2) - 2H^+ = 1900.0$ Da and $(869.0 \times 2) - 2H^+ = 1736.0$ Da were the masses of the labeled and control peptides originating from the inactivated and control enzymes, respectively. A search of the primary amino acid sequence of β-Gal Xmn for a peptide of mass 1736 ± 2 Da revealed several candidate sequences that contain an Asp or Glu residue, either of which could potentially act as the nucleophile, based on the conservation of such catalytic residues in other glycoside hydrolases. The number of peptides that could possibly contain the catalytic nucleophile was narrowed to two overlapping candidate fragments (^{248}IKFRPDQPRMVGEY^{261} and ^{258}VGEYWAGWFDHWGK^{271}) by the comparison of the β-Gal Xmn peptides of mass 1736 Da to those fragments identified through the same analysis of β-Gal-3 Bcir. Upon digestion of inactivated β-Gal-3 Bcir, comparison of the m/z profiles of the separated peptides originating from the control and inactivated enzyme samples revealed labeled and control peptides having m/z values of 1025.5 and 861.5 Da, respectively. The difference between these m/z values is 164 Da, which is within error of the expected mass difference showing that these peptides are singly charged. A search of the primary sequence of β-Gal-3 Bcir for peptides with a mass of 861 ± 2 Da indicated, again, several peptides that could potentially contain the catalytic nucleophile. Comparison of the 1736 ± 2 Da peptides of β-Gal Xmn and the 861 ± 2 Da peptides of β-Gal-3 Bcir indicated that there was only one residue with the requisite carboxylic acid side chain that appeared in at least one of the potential fragments for each enzyme and was conserved between the two glycosidases (with respect to the full sequences): Glu^{260} for β-Gal Xmn, and Glu^{233} for β-Gal-3 Bcir.

Confirmation of the identity of the position of the nucleophile of β-Gal Xmn was achieved through further analysis of the m/z 951.0 and 869.0 ions of the labeled and control peptides, respectively, by tandem mass spectrometry in the daughter ion scan mode.

The MS–MS profile of the labeled peptide shown in Fig. 5 is consistent with the expected

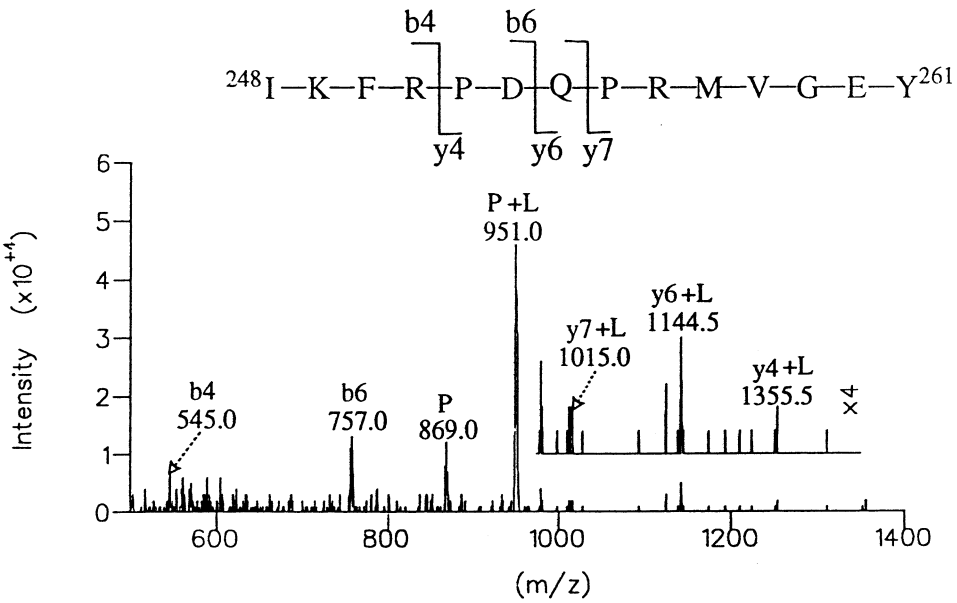

Fig. 5. Tandem MS analysis in the daughter ion scan mode of the parent m/z 951.0 peptide of labeled β-Gal Xmn. P corresponds to the full sequence depicted above and L represents the covalently bound 2-deoxy-2-fluorogalactosyl moiety. Inset shows a 4 × expansion of the region from m/z 975–1350.

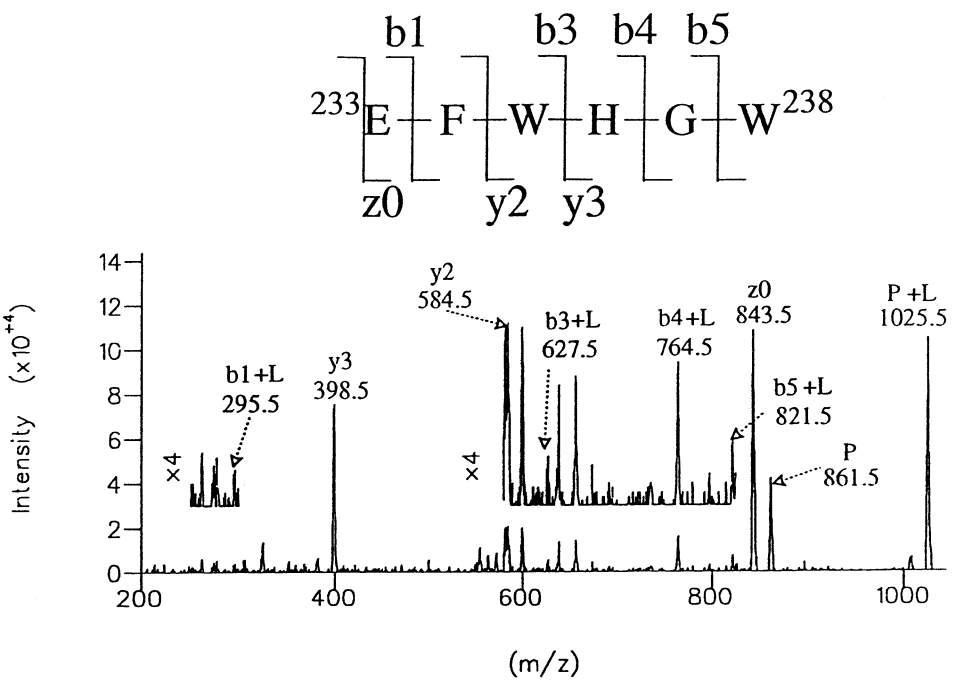

Fig. 6. Daughter ion scan of the labeled peptide of m/z 1025.5 Da originating from β-Gal-3 Bcir. Insets show 4 × expansion of the regions from m/z 250–300 to 580–825.

fragmentation pattern for the sequence ^{248}IKFRPDQPRMVGEY^{261} with the fluorogalactosyl moiety bound to a residue within the fragment PRMVGEY. As Glu^{260} is the only residue with the requisite carboxylic acid side chain within this sequence, it was concluded that this amino acid functioned as the catalytic nucleophile of β-Gal Xmn.

Similarly, the MS–MS fragmentation pattern of the 1025.5 Da labeled peptide of β-

Gal-3 Bcir (Fig. 6) is consistent with that expected for the sequence ^{233}EFWHGW^{238} with the fluoro-galactosyl moiety bound to Glu^{233}.

4. Conclusions

The experimental identification of Glu^{260} and Glu^{233} as the catalytic nucleophiles of β-Gal Xmn and β-Gal-3 Bcir, respectively, confirms the previous prediction of the location of these residues that was based on primary sequence similarities. These findings are the second and third such assignments of mechanistically important residues from the enzymes of glycoside hydrolase family 35 and essentially confirm the alignments for this diverse set of enzymes. Work is currently underway to investigate the use of β-Gal Xmn and β-Gal-3 Bcir as glycosynthases.

Acknowledgements

We thank Dr Christopher Taron of the Department of Biochemistry, University of Illinois at Urbana-Champaign, for the generous gift of the β-Gal Xmn gene. We also thank Karen Rupitz for technical assistance and the Protein Engineering Network of Centers of Excellence of Canada for financial support.

References

1. Koshland, D. E. *Biol. Rev.* **1953**, *28*, 416–436.
2. Sinnott, M. L. *Chem. Rev.* **1990**, *90*, 1171–1202.
3. Sakai, K.; Katsumi, R.; Ohi, H.; Usui, T.; Ishido, Y. *J. Carbohydr. Chem.* **1992**, *11*, 553–565.
4. Usi, T.; Kubota, S.; Ohi, H. *Carbohydr. Res.* **1993**, *244*, 315–323.
5. Prade, H.; Mackenzie, L. F.; Withers, S. G. *Carbohydr. Res.* **1998**, *305*, 371–381.
6. Vocadlo, D. J.; Withers, S. G. In *Carbohydrates in Chemistry and Biology*; Ernst, B.; Hart, G. W.; Sinay, P., Eds. Glycoside-catalyzed oligosaccharide synthesis.; Wiley-VCH: Weinheim, Germany, 2000; Vol. 2, pp. 723–844.
7. Mackenzie, L. F.; Wang, Q.; Warren, R. A. J.; Withers, S. G. *J. Am. Chem. Soc.* **1998**, *120*, 5583–5584.
8. Malet, C.; Planas, A. *FEBS Lett.* **1998**, *440*, 208–212.
9. Mayer, C.; Zechel, D. L.; Reid, S. P.; Warren, R. A. J.; Withers, S. G. *FEBS Lett.* **2000**, *466*, 40–44.
10. Fort, S.; Boyer, V.; Greffe, L.; Davies, G. J.; Moroz, O.; Chistiansen, L.; Schülein, M.; Cottaz, S.; Driguez, H. *J. Am. Chem. Soc.* **2000**, *122*, 5429–5437.
11. Withers, S. G.; Rupitz, K.; Street, I. P. *J. Biol. Chem.* **1988**, *263*, 7929–7932.
12. McCarter, J. D.; Withers, S. G. *J. Am. Chem. Soc.* **1996**, *118*, 241–242.
13. McCarter, J. D.; Burgoyne, D. L.; Miao, S.; Zhang, S.; Callahan, J. W.; Withers, S. G. *J. Biol. Chem.* **1997**, *272*, 396–400.
14. Tull, D.; Withers, S. G.; Gilkes, N. R.; Kilburn, D. G.; Warren, R. A. J.; Aebersold, R. *J. Biol. Chem.* **1991**, *266*, 15621–15625.
15. McCarter, J. D.; Withers, S. G. *J. Biol. Chem.* **1996**, *271*, 6889–6894.
16. Mackenzie, L. F.; Brooke, G. S.; Cutfield, J. F.; Sullivan, P. A.; Withers, S. G. *J. Biol. Chem.* **1997**, *272*, 3161–3167.
17. Zechel, D. L.; He, S.; Dupont, C.; Withers, S. G. *Biochem. J.* **1998**, *336*, 139–145.
18. Wong-Madden, S. T.; Landry, D. *Glycobiology* **1995**, *5*, 19–28.
19. Taron, C. H.; Benner, J. S.; Hornstra, L. J.; Guthrie, E. P. *Glycobiology* **1995**, *5*, 603–610.
20. Ito, Y.; Sasaki, T. *Biosci. Biotech. Biochem.* **1997**, *61*, 1270–1276.
21. Henrissat, B. *Biochem. J.* **1991**, *280*, 309–316.
22. Henrissat, B.; Bairoch, A. *Biochem. J.* **1993**, *293*, 781–788.
23. Henrissat, B.; Callebaut, I.; Fabrega, S.; Lehn, P.; Mornon, J. P.; Davies, G. *Proc. Natl. Acad. Sci. USA* **1995**, *92*, 7090–7094.
24. Nishimoto, J.; Nanba, E.; Inui, K.; Okada, S.; Suzuki, K. *Am. J. Hum. Genet.* **1991**, *49*, 566–574.
25. Gutshall, K.; Wang, K.; Brenchley, J. E. *J. Bacteriol.* **1997**, *179*, 3064–3067.
26. Redenbach, M.; Kieser, H. M.; Denapaite, D.; Eichner, A.; Cullum, J.; Kinashi, H.; Hopwood, D. A. *Mol. Microbiol.* **1996**, *21*, 77–96.
27. Fujimoto, H. *J. Carbohydr. Chem.* **1997**, *16*, 967–970.
28. Fujimoto, H.; Miyasato, M.; Ito, Y.; Sasaki, T.; Ajisaka, K. *Glycoconjugate J.* **1998**, *15*, 155–160.
29. Hedbys, L.; Johansson, E.; Mosbach, K.; Larsson, P. O.; Gunnarsson, A.; Svensson, S.; Lönn, H. *Glycoconjugate J.* **1989**, *6*, 161–168.
30. Altschul, S. F.; Madden, T. L.; Schäffer, A. A.; Zhang, J.; Zhang, Z.; Miller, W.; Lipman, D. J. *Nucleic Acids Res.* **1997**, *25*, 3389–3402.
31. Leatherbarrow, R. J. GRAFIT, version 3.03; Erithacus Software Ltd., 1994.
32. Pospiech, A.; Neumann, B. *Trends Genet.* **1995**, *11*, 217–218.
33. Yanish-Perron, C.; Vierira, J.; Messing, J. *Gene* **1985**, *33*, 103–119.
34. Kempton, J. B.; Withers, S. G. *Biochemistry* **1992**, *31*, 9961–9969.
35. Pace, N. C.; Vajdos, F.; Fee, L.; Grimsely, G.; Gray, T. *Protein Sci.* **1995**, *4*, 2411–2423.
36. Street, I. P.; Kempton, J. B.; Withers, S. G. *Biochemistry* **1992**, *31*, 9970–9978.